

Energy consumption and net CO₂ sequestration of aqueous mineral carbonation

W.J.J. Huijgen

G.J. Ruijg

R.N.J. Comans

G.J. Witkamp (TU Delft)

Published in Industrial & Engineering Chemistry Research 45(26), 9184-9194

Energy Consumption and Net CO₂ Sequestration of Aqueous Mineral Carbonation

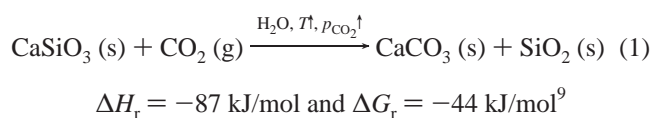
Wouter J. J. Huijgen,[†] Gerrit Jan Ruijg,[†] Rob N. J. Comans,^{*,†,‡} and Geert-Jan Witkamp[§]

Energy Research Centre of The Netherlands, P.O. Box 1, 1755ZG Petten, The Netherlands, Department of Soil Quality, Wageningen University, P.O. Box 8005, 6700EC Wageningen, The Netherlands, and Laboratory for Process Equipment, Delft University of Technology, Leeghwaterstraat 44, 2628CA Delft, The Netherlands

Aqueous mineral carbonation is a potentially attractive sequestration technology to reduce CO₂ emissions. The energy consumption of this technology, however, reduces the net amount of CO₂ sequestered. Therefore, the energetic CO₂ sequestration efficiency of aqueous mineral carbonation was studied in dependence of various process variables using either wollastonite (CaSiO₃) or steel slag as feedstock. For wollastonite, the maximum energetic CO₂ sequestration efficiency within the ranges of process conditions studied was 75% at 200 °C, 20 bar CO₂, and a particle size of <38 μm. The main energy-consuming process steps were the grinding of the feedstock and the compression of the CO₂ feed. At these process conditions, a significantly lower efficiency was determined for steel slag (69%), mainly because of the lower Ca content of the feedstock. The CO₂ sequestration efficiency might be improved substantially for both types of feedstock by, e.g., reducing the amount of process water applied and further grinding of the feedstock. The calculated energetic efficiencies warrant a further assessment of the (energetic) feasibility of CO₂ sequestration by aqueous mineral carbonation on the basis of a pilot-scale process.

1. Introduction

Mineral carbonation is a potentially attractive CO₂ sequestration technology to mitigate possible climate change, on the basis of industrially mimicked natural weathering processes.^{1–3} Potential feedstocks for mineral CO₂ sequestration include primary Ca/Mg-silicates, such as wollastonite (CaSiO₃)^{4,5} and olivine (Mg₂SiO₄),^{5,6} and industrial residues, such as steel slag⁷ and waste cement.⁸ A number of different process routes have been reported, of which the aqueous mineral carbonation route was selected as the most promising in a recent review² (see also references therein), e.g., for wollastonite:



The key issue in mineral carbonation research is the enhancement of the carbonation reaction, which is typically very slow at natural conditions.^{2,3} In previous papers, we have studied the aqueous carbonation of two Ca-silicates, wollastonite⁴ and steel slag,^{7,10} and shown that the carbonation rate could be increased significantly by, e.g., grinding the feedstock and elevating the temperature and CO₂ pressure in the process. The process conditions required for substantial conversion seem technically feasible (i.e., typically, 175–200 °C, 10–40 bar CO₂, a particle size of <38 μm, and a reaction time of 15–30 min). However, all the measures required to increase the reaction rate consume energy and reduce the net amount of CO₂ sequestered because of extra CO₂ emissions caused. On the other hand, the exothermic mineral carbonation reaction may potentially generate usable heat. Overall, an energetic CO₂ sequestration ef-

iciency (η_{CO_2}) of the mineral carbonation process can be defined on the basis of the amount of CO₂ sequestered in the carbonation reactor (CO_{2,sequestered}) and the net overall amount of CO₂ sequestered by the mineral carbonation process (CO_{2,avoided}):

$$\eta_{\text{CO}_2} [\%] = \frac{\text{CO}_{2,\text{avoided}}}{\text{CO}_{2,\text{sequestered}}} \times 100 = 100 - \frac{E_{\text{power}}\epsilon_{\text{power}} + E_{\text{heat}}\epsilon_{\text{heat}}}{\text{CO}_{2,\text{sequestered}}} \times 100 \quad (2)$$

The extra CO₂ emissions associated with the mineral carbonation process are determined by the power and heat consumption of the process (taking the reaction heat into account) (E_{power} and E_{heat} , respectively) and the conversion factors of the power and heat consumption into CO₂ emissions (ϵ_{power} and ϵ_{heat} , respectively). The energy consumption of the mineral carbonation process is influenced by the conditions in the carbonation reactor both directly as well as indirectly through their effect on the carbonation conversion. Therefore, a system study of the aqueous mineral carbonation process is required to determine its overall energetic CO₂ sequestration efficiency and to optimize this efficiency on the basis of its dependence on the reactor conditions.

A number of (preliminary) system studies on different approaches for CO₂ sequestration by mineral carbonation have been published, e.g., refs 5, 11, and 12, including the aqueous mineral carbonation route.⁵ However, the results presented for wollastonite in the latter system study by the Albany Research Center (ARC) have been predicted on the basis of a carbonation process designed for olivine. In addition, the study does not include the use of industrial residues as feedstock for mineral carbonation. Although their availability is relatively limited, residues might be of interest since no mining is required and residues tend to be more reactive with regard to carbonation than ores at relatively mild process conditions.^{4,7}

The aim of the present study is to determine and optimize the energetic performance of CO₂ sequestration by aqueous

* Corresponding author. Phone: +31 224564218. Fax: +31 224568163. E-mail: comans@ecn.nl.

[†] Energy Research Centre of The Netherlands.

[‡] Wageningen University.

[§] Delft University of Technology.

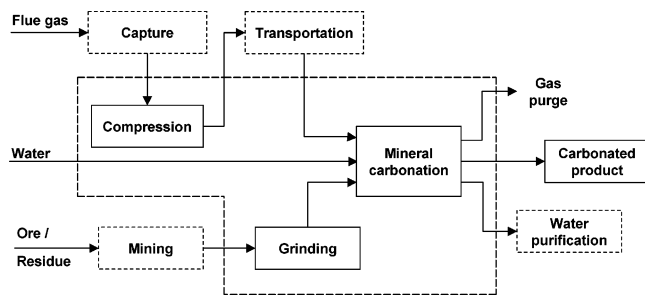


Figure 1. Block diagram of mineral carbonation process for CO₂ sequestration together with system boundaries of the present study.

carbonation of Ca-silicates, both an ore and an industrial residue. A mineral carbonation process will be designed and the CO₂ sequestration efficiency will be determined at various sets of process conditions. A sensitivity analysis will be performed in order to assess the accuracy of the energetic efficiency determined and to indicate routes for further improvement of the CO₂ sequestration efficiency.

2. Methods and Assumptions

2.1. Process Simulation. A block diagram of a CO₂ sequestration process on the basis of mineral carbonation is shown in Figure 1 including the system boundaries of the present study. The mineral carbonation plant is assumed to be located at the source of the solid feedstock. The mineral carbonation process step, which is subject of this study, includes the compression of the CO₂ feed and the grinding of the feedstock (Figure 1). ASPEN Plus flow-sheeting software¹³ was used to simulate the continuous mineral carbonation process, for which the flowsheet is shown in Figure 2. In the process, the solid feedstock, after being ground to a specific particle size (d) (Section 2.2), is mixed with water at a specific liquid-to-solid ratio (L/S), and the resulting slurry is pumped to the reactor pressure (p). Subsequently, the slurry is heated with the carbonation reactor outlet in a heat exchanger to 20 °C below the reactor temperature (T). CO₂ is pressurized in a multiple-stage compressor to the reactor pressure and added to the slurry. The mixture is heated to the reactor temperature, and the carbonation reaction takes place in a continuous (cooled) carbonation reactor at isothermal conditions during the reaction time (t). The total pressure in the reactor equaled the sum of the partial CO₂ pressure (p_{CO_2}) and the H₂O vapor pressure ($p_{\text{H}_2\text{O}}$) as determined by ASPEN at the reactor temperature (e.g., $p_{\text{H}_2\text{O}} = 16$ bar at 200 °C). After the reactor, the nonreacted gaseous CO₂ is separated from the solid–liquid slurry and recycled to the reactor. The slurry is depressurized to 1 atm after being cooled to 40 °C in two steps (first, in a heat exchanger by exchanging heat with the reactor feed and, second, in a cooler with cooling water). The CO₂ released from the slurry upon depressurization is recycled to the compressor in a second CO₂ recycle. The solid product is separated from the slurry by filtration, and the remaining process water is recycled. A purge is used in both the liquid and the main gas recycles to avoid possible accumulation of (inert) impurities (i.e., soluble salts leached from the feedstock and gaseous impurities in the (captured) CO₂ feed, such as N₂). In the compressor, moisture present in the second CO₂-recycle stream might condense. This condensate is separated and added to the water recycle. Table 1 shows additional assumptions used for the various unit operations.

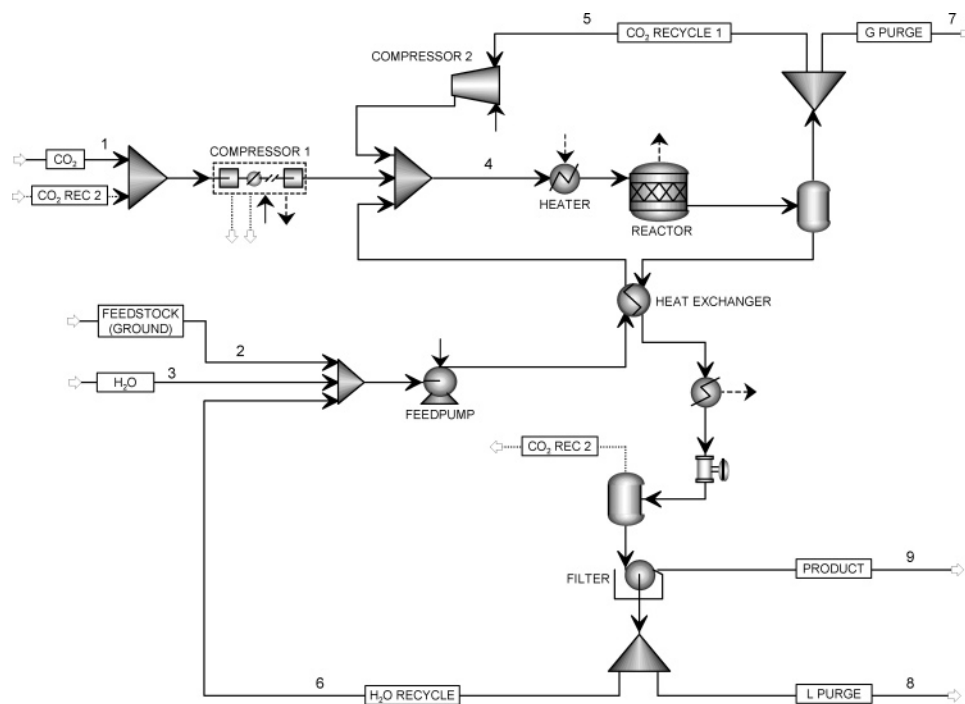
The thermodynamic property set used for the ASPEN simulations, “Peng–Robinson with Huron–Vidal 2 mixing

rules” (PRMHV2), was selected according to Carlson¹⁴ on the basis of a polar nonelectrolyte system at pressures > 10 bar. The influence of ions (generated by leaching from solids and dissolution of gaseous CO₂) on the thermodynamic properties of the system was neglected. However, the effect of dissolved ions on the carbonation reaction^{4,7} is implicitly included in the definition of the conversion in the carbonation reactor (Section 2.3). The ASPEN components defined for the wollastonite carbonation process were “carbon-dioxide” (CO₂), “water” (H₂O), and the solids “wollastonite” (CaSiO₃), “silicon-dioxide” (SiO₂), and “calcium-carbonate-calcite” (CaCO₃). The composition used for the wollastonite feedstock was 84.3 wt % CaSiO₃, 13.9 wt % SiO₂, and 1.8 wt % CaCO₃,⁴ assuming all other (inert) components were present as SiO₂. The only reaction taken into account was the carbonation reaction (eq 1), which was assumed to occur exclusively in the carbonation reactor (see Section 2.3). The steel slag feedstock consisted mainly of Ca and Fe phases.⁷ In previous work, the various Ca phases and their carbonation reactions have been identified.^{7,10} However, the contribution of each phase and reaction could not be quantified. Therefore, as a simplification, the composition of the steel slag⁷ was defined in terms of the same Ca components as used for wollastonite plus “ferrous-oxide” (FeO) (56.8 wt % CaSiO₃, 7.7 wt % CaCO₃, and 35.5 wt % FeO). It was assumed that all Ca was present as either CaSiO₃ or CaCO₃ (based on the carbonate content in Section 2.3) and that the rest of the feedstock consisted of FeO. FeO was considered to be inert, since no significant amount of carbonate minerals other than calcite was formed at the process conditions applied in the steel slag carbonation experiments.⁷ Analogously to wollastonite, the Ca carbonation reaction of steel slag was assumed to be represented by eq 1 (see also Section 3.3.4).

2.2. Feedstock Batches. Table 2 shows the definition of the wollastonite and steel slag feedstock batches used in this study. For each batch, the corresponding power required for grinding (W) was calculated with Bond’s equation,¹⁵

$$W = 0.01 W_i \left(\frac{1}{\sqrt{d_1}} - \frac{1}{\sqrt{d_0}} \right) \quad (3)$$

with the original particle size of the feedstock (d_0), the imaginary sieve size through which 80 wt % of the ground feedstock passes (d_1), and the standard Bond’s working index (W_i) (as reported in the literature for $d_0 = \infty$ and $d_1 = 100 \mu\text{m}$)¹⁶). In the case of a grinding step with final particle size < 70 μm , an extra multiplier of $(10.6 \times 10^{-6} + d_1)/1.145d_1$ was applied to eq 3, as used by ASPEN¹³ (see also ref 16). The fresh wollastonite ore was assumed to be supplied to the grinding equipment as uniform particles of 0.1 m (d_0). The standard Bond’s working index (W_i) of wollastonite was set at 14 kWh/ton (i.e., mean of working indices of limestone (11.6 kWh/ton) and silica sand (16.5 kWh/ton))¹⁶). The ore grade of the wollastonite ore was assumed to be 50%.⁵ Following the approach taken by the Albany Research Center,⁵ the wollastonite ore was assumed to be first ground to <200 mesh (roughly 75 μm) and, subsequently, concentrated to the composition assumed for the wollastonite feedstock by removing the gangue (see Section 2.1). Finally, the concentrated ore is ground to its final particle size. If the final particle size is >75 μm , grinding was performed in a single step. The energy penalty for the beneficiation (i.e., ore concentrating) step was assumed to be 4 kWh/ton.⁵ Because ore grade is no issue for steel slag, this feedstock is ground in a single step. For this material, the standard Bond’s working index available for blast furnace slag of 12 kWh/ton¹⁶ was used.



Stream number	1	2	3	4	5	6	7	8	9
<i>Wollastonite</i>									
T [°C]	25	25	25	180	200	39	40	39	39
p [bar]	1.0	1.0	1.0	35.5	34.5	1.0	1.0	1.0	1.0
Mass flow [ton/ton CO ₂ seq]									
CaSiO ₃		3.8		3.8					1.2
CaCO ₃		0.1		0.1					2.4
SiO ₂		0.6		0.6					2.0
H ₂ O			1.0	22.7	0.0	21.6	0.0	0.0	1.0
CO ₂	1.0			1.8	0.1	0.3	0.0	0.0	0.0
<i>Steel slag</i>									
T [°C]	25	25	25	181	200	39	40	39	39
p [bar]	1.0	1.0	1.0	35.5	34.5	1.0	1.0	1.0	1.0
Mass flow [ton/ton CO ₂ seq]									
CaSiO ₃		3.9		3.9					1.3
CaCO ₃		0.5		0.5					2.8
SiO ₂									1.4
FeO		2.4		2.4					2.4
H ₂ O			1.4	34.4	0.0	33.0	0.0	0.0	1.4
CO ₂	1.0			1.7	0.1	0.4	0.0	0.0	0.0

Figure 2. Simplified ASPEN flow diagram of an aqueous mineral carbonation process. At the points indicated, the temperature, pressure, and composition of streams are given in the table. Process conditions: $T = 200$ °C, $p_{\text{CO}_2} = 20$ bar, batches W1 and S1 ($d < 38$ μm), and $L/S = 5$ kg/kg ($\zeta_{\text{CaSiO}_3} = 69\%$ and 67% for wollastonite and steel slag, respectively). Heat (solid-line arrow) and power (dashed-line arrow) flows are indicated.

In addition, a particle size of 0.02 m was selected as a representative size for freshly produced steel slag. The 80 wt % passing size of the individual wollastonite and steel slag batches was estimated on the basis of the particle size distribution measured by laser diffraction^{4,7} (Table 2).

2.3. Carbonation Degree. The conversion in the carbonation reactor defined the required supply of fresh solid feedstock (i.e., the amount of CO₂ sequestered is fixed; see Table 1). The influence of the following six process variables on the carbonation degree (ζ) had been studied previously in a lab-scale autoclave reactor for both wollastonite and steel slag: temperature, CO₂ pressure, particle size, stirring rate (n), residence time, and liquid-to-solid ratio.^{4,7} These data sets were applied as an estimation of the conversion in the continuous large-scale carbonation reactor used in this system study. For simulation purposes, the Ca carbonation degree as measured in the lab-scale autoclave reactor (ζ_{Ca})^{4,7} was ex-

pressed in terms of the CaSiO₃ fraction in the reactor inlet (ζ_{CaSiO_3}). In the case of steel slag, conversion data reported earlier⁷ were first corrected for the carbonate content of the fresh steel slag (3.4 wt %) similarly to the approach reported for wollastonite.⁴

For the specific purpose of this system study, three series of additional carbonation experiments were performed in the autoclave reactor following the experimental approach described earlier.^{4,7} For these additional experiments, two extra feedstock batches were prepared and analyzed as reported in previous work^{4,7} (batches W2 (< 106 μm) and S2 (< 38 μm); see Table 2). In the first series of experiments, steel slag was carbonated in duplicate at the same process conditions at which the maximum energetic efficiency was found for wollastonite (see Section 3.1; $d < 38$ μm , $T = 200$ °C, $p_{\text{CO}_2} = 20$ bar, $t = 15$ min, $n = 500$ rpm, and $L/S = 5$ kg/kg). In the other two series of experiments, the effect of process water recycling on the

Table 1. Assumptions Used within the ASPEN Simulations for the Unit Operations

unit operation	assumptions
pump	pump efficiency = 0.8; single-stage centrifugal pump
compressor 1	three-stage centrifugal compressor with intermediate cooling between subsequent stages to 40 °C; ^a isentropic operation with an efficiency of 0.8 for each stage; condensed water added to process water recycle
compressor 2	single-stage blower; isentropic operation with an efficiency of 0.8
reactor	isothermal operation; pressure drop = 1 bar; amount of CO ₂ sequestered = 1 ton/h ^b
filter	centrifugal filter; atmospheric operation; separation efficiency of solids = 100%; mass fraction of solids in cake = 0.85
flash drums	isothermal and isobaric; top flash carbonation reactor outlet = 0.1 ton/h of CO ₂ ^c
valves	adiabatic operation
splitters ^d	0% purge fractions for both CO ₂ recycle 1 and H ₂ O recycle
other	all starting materials enter the process at 25 °C and 1 atm; product and purge streams leave the process at 1 atm

^a The number of stages is selected such that the pressure ratio per stage for the highest outlet pressure simulated (i.e., 65.5 bar) is between 3:1 and 5:1.¹⁶ ^b The difference between the amount of CO₂ present in the reactor in- and outlet. Only defined for simulation purposes, since the CO₂ sequestration efficiency is independent of the scale of the process. ^c At the end of the carbonation reaction, remaining gaseous CO₂ has to be present in the reactor outlet to ensure that the slurry in the reactor has been saturated with dissolved CO₂ during the entire carbonation reaction. Therefore, 10% of the amount of CO₂ sequestered in the reactor was specified to come over the top in the flash after the reactor. ^d In a final plant design, the CO₂ purge fraction is determined by the composition of the gas stream resulting after CO₂ capture. The H₂O purge fraction depends on the composition of the water recycle stream. Both are yet unknown, and the purge fractions are, therefore, set at 0.

Table 2. Definition, Particle Size Data, and Grinding Energy of Wollastonite and Steel Slag Feedstock Batches

batch	sieve [μm]	D[4,3] ^a [μm]	d ₁ ^b [μm]	W ^c [kWh/ton of feedstock]			
				G-1	B	G-2	total
wollastonite							
W1	<38	16	20	31 ^d	4 ^e	20 ^f	56
W2	<106	45	60	31	4	3	38
W3	<106	51	69	31	4	1	36
W4	<500	159	240	17	4		21
W5	<7000	375	631	10	4		14
steel slag							
S1	<38	14	23				31 ^g
S2	<38	15	23				31
S3	<106	33	52				17
S4	<106	34	52				17
S5	<500	97	158				9
S6	<2000	582	832				3

^a Volume-based mean particle size. ^b 80 wt % passing sieve size (see eq 2). ^c W = grinding energy. In the case of wollastonite, the grinding energy consists of three steps: first-stage grinding (G-1), beneficiation (B), and second-stage grinding of the concentrated ore (G-2). In the case of steel slag, grinding takes place in a single step. ^d First grinding step from 0.1 m to 75 μm; ore grade = 50%; W_i = 14 kWh/ton. ^e Energy penalty for beneficiation. ^f Second grinding step from 75 μm to final particle size; W_i = 14 kWh/ton. ^g d₀ = 0.02 m and W_i = 12 kWh/ton.¹⁶

carbonation degree and the composition of the process water was studied for both wollastonite and steel slag (see Supporting Information).

2.4. CO₂ Sequestration Efficiency. For each set of reactor conditions, the ASPEN flowsheet of the mineral carbonation process as given in Figure 2 was simulated. The outcome consisted of the composition, temperature, and pressure of the process streams and the power and heat consumption of the

unit operations. Subsequently, the CO₂ sequestration efficiency was calculated on the basis of eq 2. The power consumption of the mineral carbonation process (E_{power}) consisted of power consumption for compression, pumping, and grinding. The (possible) power consumption of the reactor and the filter were neglected. E_{heat} was the net process heat (i.e., the heat required for heating the reactants minus the reaction heat). In the case of a possible surplus of process heat, a useful application of this heat was assumed outside the system boundaries of this study and the negative CO₂ emissions associated were taken into account in the energetic CO₂ efficiency. The reaction heat of the carbonation reaction (eq 1) was calculated by ASPEN for each reactor temperature and pressure (e.g., -84 kJ/mol at standard conditions). The conversion factor of the power required in the process into CO₂ emissions (ϵ_{power}) was set at 0.60 (kg of CO₂)/kWh as an estimation of the average value in The Netherlands (cf. representative values for a natural gas combined cycle and a powder coal power plant of 0.36 and 0.80 (kg of CO₂)/kWh, respectively¹⁷). The conversion factor of the heat consumption in the process into CO₂ emissions was based on the combustion of methane ($\Delta H_{\text{r}} = -803$ kJ/mol¹⁶ or $\epsilon_{\text{heat}} = 0.20$ kg CO₂/kWh).

In the simulations, the influence of the process variables reactor temperature, CO₂ partial pressure, and particle size on the CO₂ sequestration efficiency was studied. The ranges within which these variables could be varied were slightly restricted compared to the carbonation experiments.⁴ Because of the pressure drop over the reactor (1 bar), simulations on the basis of carbonation measurements at $p_{\text{CO}_2} = 1$ bar were performed with $p_{\text{CO}_2} = 1.5$ bar to enable simulation. In addition, processes with a reactor temperature below 60 °C could not be simulated because of the assumptions given in Table 1 ($T_{\text{H}_2\text{O}-\text{recycle}} = 40$ °C and $\Delta T_{\text{heat-exchanger}} = 20$ °C).

The possible influence on the CO₂ sequestration efficiency of the other process variables studied experimentally, i.e., residence time, agitation rate, and L/S ratio,^{4,7} was (initially) not taken into account in this study. A longer residence time increases the energy consumption of the process that must be kept at elevated temperature and pressure for a longer time. However, these energy losses are not taken into account in the current assessment, since they cannot be quantified at the current stage of process development. The possible minimum agitation rate and the accompanying power input required to obtain sufficient mixing in the continuous carbonation reactor are also currently unknown. For reasons of comparison, all wollastonite and steel slag simulations were (initially) performed at $L/S = 5$ kg/kg, although the steel slag conversions were actually measured at $L/S = 10$ kg/kg.⁷ The consequences of this assumption will be discussed in Section 3.3. The L/S ratio was defined in the ASPEN flowsheet on the basis of all solids present in the reactor feed.

Finally, a sensitivity analysis was performed on the CO₂ sequestration efficiency of aqueous wollastonite carbonation at the energetically optimum reactor conditions (Section 3.1). In this analysis, a selection of assumptions and input variables for the ASPEN simulations and the CO₂ emission calculations were varied within possible limits. For steel slag, a similar analysis was performed at identical conditions.

3. Results and Discussion

3.1. Wollastonite. Figure 3 shows the influence of the particle size, reactor temperature, and CO₂ pressure on (1) the measured carbonation degree of wollastonite,⁴ expressed in terms of the CaSiO₃ fraction in the reactor feed (ζ_{CaSiO_3}), and (2) the

Wollastonite

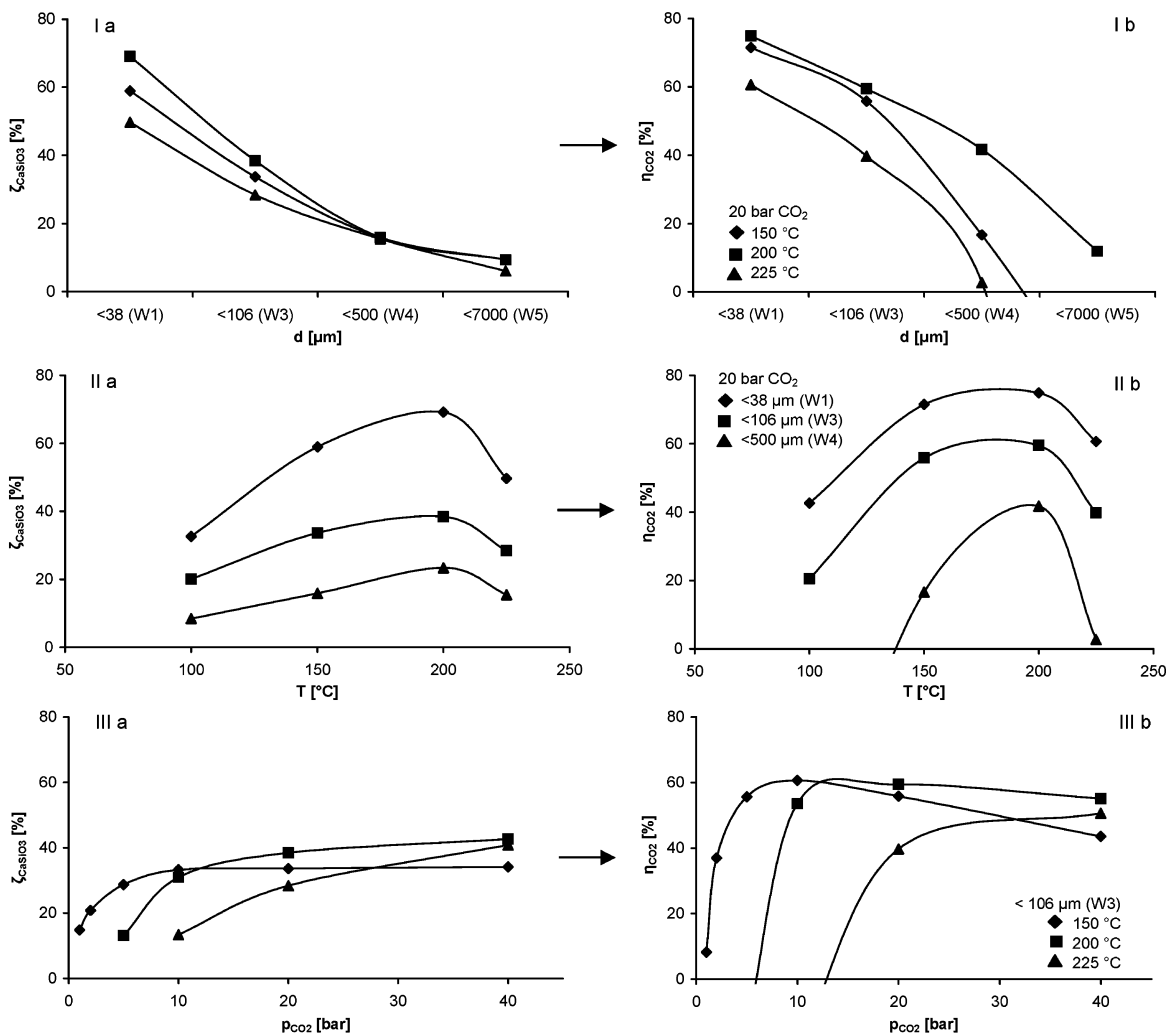


Figure 3. Measured carbonation degree (ζ_{CaSiO_3})⁴ and the corresponding calculated CO₂ sequestration efficiency (η_{CO_2}) as a function of various process variables for wollastonite. Simulations were performed at $L/S = 5$ kg/kg. Conversion measurements in lab-scale autoclave reactor were performed at $t = 15$ min, $n = 500$ rpm, and $L/S = 5$ kg/kg. (I) Particle size at various reactor temperatures; (II) reactor temperature at various particle sizes; and (III) CO₂ pressure at various temperatures.

corresponding simulated CO₂ sequestration efficiencies (η_{CO_2}). In general, differences between the ζ_{CaSiO_3} and η_{CO_2} curves appear at low carbonation degrees, since a low conversion has a strong reducing effect on the sequestration efficiency. Substantially more energy is required for both grinding the feedstock and heating the wollastonite–water slurry.

The influence of process variables on the energetic sequestration efficiency shown in Figure 3 consists of a direct effect of the process variables on the energy consumption as well as an indirect effect through their influence on the carbonation degree. To be able to distinguish between both effects, Table 3 shows the influence of the same process variables on the sequestration efficiency at constant conversion (arbitrarily kept at 69%; see below). It should be noted that the simulations presented in Table 3 are performed for the specific purpose of eliminating the *indirect* effect of the process conditions on the energetic efficiency, thus allowing an assessment of only the *direct* effect of these conditions on the energy consumption.

Figure 3.I.b shows that increasing the conversion by size reduction is favorable with regard to the CO₂ sequestration efficiency, within the ranges of process conditions studied ($d = <38 - <7000 \mu\text{m}$). Grinding leads to a higher carbonation

degree because of an increased specific surface area⁴ and, thereby, a reduction of the amount of feedstock that has to be processed (Figure 3.I.a). On the other hand, the grinding energy per kilogram of feedstock increases substantially for smaller particle sizes (Table 2), which has a reducing effect on the energetic efficiency (Table 3). Figure 3.I.b shows that the effect of the increased conversion on the energetic efficiency is larger than the extra energy consumption, within the range of particle sizes studied. However, the cases simulated for small particle sizes are less favorable from an energetic point of view than from a conversion point of view (Figure 3.I.b), and an optimum in CO₂ sequestration efficiency probably occurs when the wollastonite is further ground to particle sizes smaller than <38 μm ($d_1 = 20 \mu\text{m}$; see Table 2).

The reactor temperature shows an optimum carbonation rate (Figure 3.II.a) and energetic efficiency (Figure 3.II.b) around 200 °C. The occurrence of a maximum carbonation degree is caused by two opposite temperature effects: (1) a higher dissolution rate of Ca upon a temperature increase and (2) a retardation of the CaCO₃ precipitation due to decreased CO₂ activity in solution.⁴ The influences of the reactor temperature on the CO₂ sequestration efficiency and the CaSiO₃ conversion

Table 3. Direct Influence of Process Variables on the Power and Heat Consumption and CO₂ Sequestration Efficiency for Wollastonite^a

variable	feedstock batch		reactor conditions				ζ_{CaSiO_3} [%]	power [kWh/ton of CO ₂ seq]		heat [kWh/ton of CO ₂ seq]		η_{CO_2} [%]
	d [μm]	T [$^{\circ}\text{C}$]	$p_{\text{H}_2\text{O}}$ [bar]	p_{CO_2} [bar]	p [bar]	I ^c		II ^d	III ^e	IV ^f		
d	W1	<38	200	16	20	36	69	253	150	-799	752	75
	W3	<106	200	16	20	36	69	165	150	-799	752	80
	W4	<500	200	16	20	36	69	96	150	-799	752	84
	W5	<7000	200	16	20	36	69	65	150	-799	752	86
p_{CO_2}	W1	<38	200	16	10	26	69	253	101	-994	934	78
	W1	<38	200	16	20	36	69	253	150	-799	752	75
	W1	<38	200	16	30	46	69	253	202	-724	690	72
	W1	<38	200	16	40	56	69	253	256	-679	658	69
T	W1	<38	100	16	20	36	69	253	367	-197	556	70
	W1	<38	150	16	20	36	69	253	225	-505	597	73
	W1	<38	175	16	20	36	69	253	185	-629	643	74
	W1	<38	200	16	20	36	69	253	150	-799	752	75
$T + p_{\text{H}_2\text{O}}$	W1	<38	100	1	20	21	69	253	198	-373	564	77
	W1	<38	150	5	20	25	69	253	151	-572	618	77
	W1	<38	175	9	20	29	69	253	147	-672	670	76
	W1	<38	200	16	20	36	69	253	150	-799	752	75

^a In the simulations, conversion is kept constant at 69%. Corresponding starting process conditions: batch W1 ($d < 38 \mu\text{m}$), $T = 200 \text{ }^{\circ}\text{C}$, and $p_{\text{CO}_2} = 20$ bar. Simulations were performed at $L/S = 5 \text{ kg/kg}$. ^b Conversion was kept constant to eliminate the indirect effect of the process conditions on the energetic efficiency through their influence on the conversion. ^c Grinding. ^d Compression + pumping. ^e Heater. ^f Reactor heat.

are similar, although the influence is less significant for the efficiency (Figure 3.II, $d < 38 \mu\text{m}$). Apparently, the extra CO₂ emissions associated with an increase of the reactor temperature to 200 °C are smaller than the extra amount of CO₂ sequestered. These extra CO₂ emissions are caused both by the increased temperature itself as well as by the temperature effect on the water vapor (and total) pressure. Table 3 shows calculations at both constant and adjusted total pressure. The influence of the temperature at constant total pressure will be discussed first.

At constant carbonation degree and water vapor pressure, a higher reactor temperature would increase the energy required to heat the CO₂ gas (Table 3). However, changing the reactor temperature has no direct effect on the energy consumption of the heater used for heating the liquid–solid slurry. The slurry is heated to 20 °C below the reactor temperature in the heat exchanger independently of the actual reactor temperature. As an indirect effect of a higher reactor temperature, the amount of dissolved CO₂ in the reactor outlet decreases because of a solubility decrease. Thus, less CO₂ is recycled in the second CO₂ recycle and would have to be recompressed (stream “CO₂ REC 2” in Figure 2). Finally, the reactor temperature affects the reactor heat (Table 3). Overall, an increase of the reactor temperature at constant total pressure and carbonation degree would have an increasing effect on the CO₂ sequestration efficiency (Table 3). Apparently, the effect on the amount of dissolved CO₂ dominates the other temperature effects.

If the temperature effect on the water vapor pressure is included (Table 3), the effects of reactor temperature and pressure on the energetic efficiency occur in combination (see below for more detail). The power required for compression shows a minimum for the 175 °C case (two countereffective effects occur: a higher energy consumption for compression due to the higher total pressure and a smaller amount of CO₂ that has to be compressed) (Table 3). Overall, elevation of the reactor temperature has a slightly decreasing direct effect on the CO₂ sequestration efficiency caused by the increase of the water vapor pressure (Table 3).

Finally, elevation of the CO₂ pressure has, in most cases, a favorable effect on the CO₂ sequestration efficiency (Figure 3.III). However, cases with only a small positive effect of the CO₂ pressure on the conversion form an exception (i.e., 150 and 200 °C lines in Figure 3.III.b). A higher CO₂ pressure, in principle, increases the carbonation degree because of an

increase of the CaCO₃ precipitation rate⁴ (Figure 3.III). However, above a specific (temperature-dependent) CO₂ pressure, the carbonation degree becomes independent of the CO₂ pressure since the (bi)carbonate activity in solution is no longer rate-limiting⁴ (Figure 3.III.a). The direct effect of a higher p_{CO_2} on the energetic efficiency consists not only of increased power consumption for compression but also of a changed heat balance of the process (Table 3). A higher CO₂ pressure increases the temperature of the CO₂ gas outlet stream of the compressor and, thus, lowers the energy consumption of the heater. In addition, the reactor heat decreases upon an increasing CO₂ pressure. The actual reactor heat of -799 kWh/(ton of CO₂ sequestered) at 200 °C and 20 bar CO₂ consists of the standard reaction heat as specified at standard conditions (-528 kWh/(ton of CO₂ sequestered) at 25 °C and 1 bar) corrected for the actual reactor temperature and pressure. The extra CO₂ emission caused by increased compression is larger than the influence of the heat balance of the process, and overall, an increase of the CO₂ pressure has a direct reducing effect on the CO₂ sequestration efficiency (Table 3). Overall, this extra CO₂ emission due to elevating the CO₂ pressure is generally smaller than the extra CO₂ sequestered at a higher CO₂ pressures (Figure 3.III). However, cases with only a small effect of a higher CO₂ pressure on the conversion might become energetically less favorable for the higher pressures (i.e., 150 and 200 °C lines in Figure 3.III.b). Therefore, the optimum CO₂ pressure can only be determined by additional carbonation experiments and simulations at the optimum reactor temperature (200 °C) and particle size.

The maximum energetic efficiency of CO₂ sequestration by wollastonite carbonation found within the ranges of process conditions studied is 75%. The corresponding set of conditions is $T = 200 \text{ }^{\circ}\text{C}$, $p_{\text{CO}_2} = 20$ bar, and $d < 38 \mu\text{m}$ with a carbonation degree (ζ_{CaSiO_3}) of 69%. In the rest of this paper, we refer to this set as the “energetically optimum” process conditions, although more favorable conditions may occur outside the range of experimental data that this study is based on. For this set of conditions, Figure 2 shows the stream properties for the aqueous wollastonite carbonation process and Table 4 shows the accompanying heat and power flows. The largest fraction of the total power required is for grinding, followed by that for compression of the CO₂ feed. The power required for recompression of the CO₂ recycle and for pumping the slurry is very

Table 4. Heat and Power Consumption of Process Equipment and Their Individual Effects on the CO₂ Sequestration Efficiency for Wollastonite (batch W1) and Steel Slag (S1)^a

process equipment	wollastonite		steel slag		
	<i>E</i> [kWh/ton of CO ₂ seq]	$\Delta\eta_{\text{CO}_2}$ [%]	<i>E</i> [kWh/ton of CO ₂ seq]	$\Delta\eta_{\text{CO}_2}$ [%]	
power	compressor 1	118 (96)	-7 (-6)	137 (104)	-8 (-6)
	compressor 2	0 (0)	-0 (-0)	0 (0)	-0 (-0)
	pump	33 (13)	-2 (-1)	50 (20)	-3 (-1)
	grinding	253 (253)	-15 (-15)	213 (213)	-13 (-13)
	sum	403 (362)	-24 (-22)	400 (337)	-24 (-20)
heat	reactor	-752 (-757)	+15 (+15)	-747 (-755)	+15 (+15)
	heater	799 (462)	-16 (-9)	1101 (588)	-22 (-12)
	sum	47 (-295)	-1 (+6)	354 (-167)	-7 (+3)
total efficiency loss		-25 (-16)		-31 (-17)	
η_{CO_2} [%]		75 (84)		69 (82)	

^a Process conditions: $d < 38 \mu\text{m}$, $T = 200 \text{ }^\circ\text{C}$, and $p_{\text{CO}_2} = 20 \text{ bar}$ [$\zeta_{\text{CaSiO}_3} = 69\%$ (wollastonite) and 67% (steel slag)]. Standard calculations were performed at $L/S = 5 \text{ kg/kg}$, and alternative calculations shown between brackets were performed at $L/S = 2 \text{ kg/kg}$. ^b CO₂ sequestration efficiency loss.

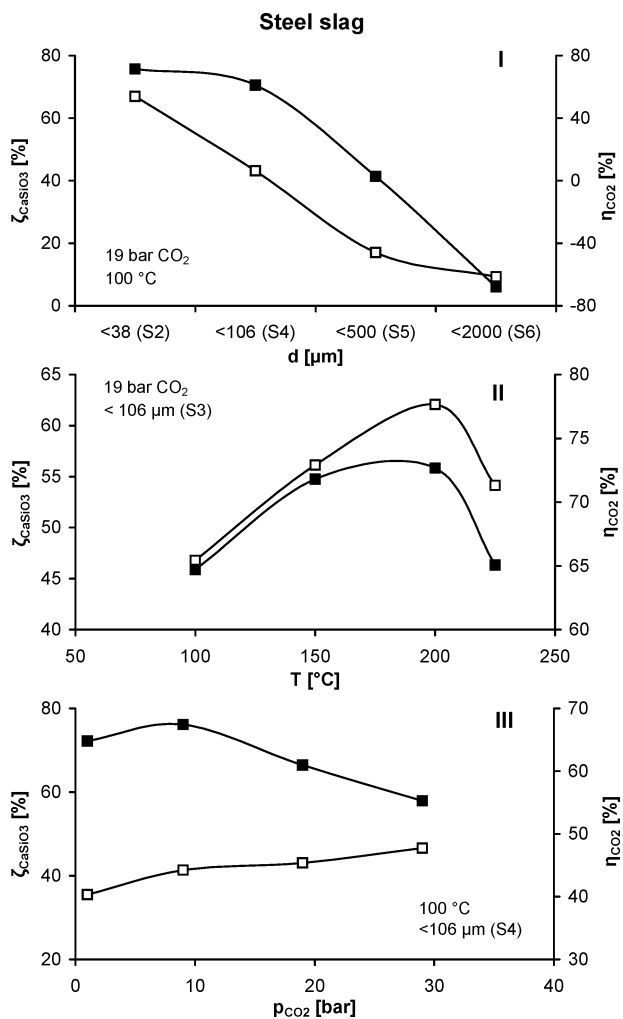


Figure 4. Measured carbonation degree (ζ_{CaSiO_3})⁷ (open symbols) and the corresponding calculated CO₂ sequestration efficiency (η_{CO_2}) (solid symbols) as a function of various process variables for steel slag. Simulations were performed at $L/S = 5 \text{ kg/kg}$. Conversion measurements in lab-scale autoclave reactor were performed at $t = 30 \text{ min}$, $n = 500$ (I)/1000 (II and III) rpm, and $L/S = 10 \text{ kg/kg}$. (I) Particle size; (II) reactor temperature; and (III) CO₂ pressure.

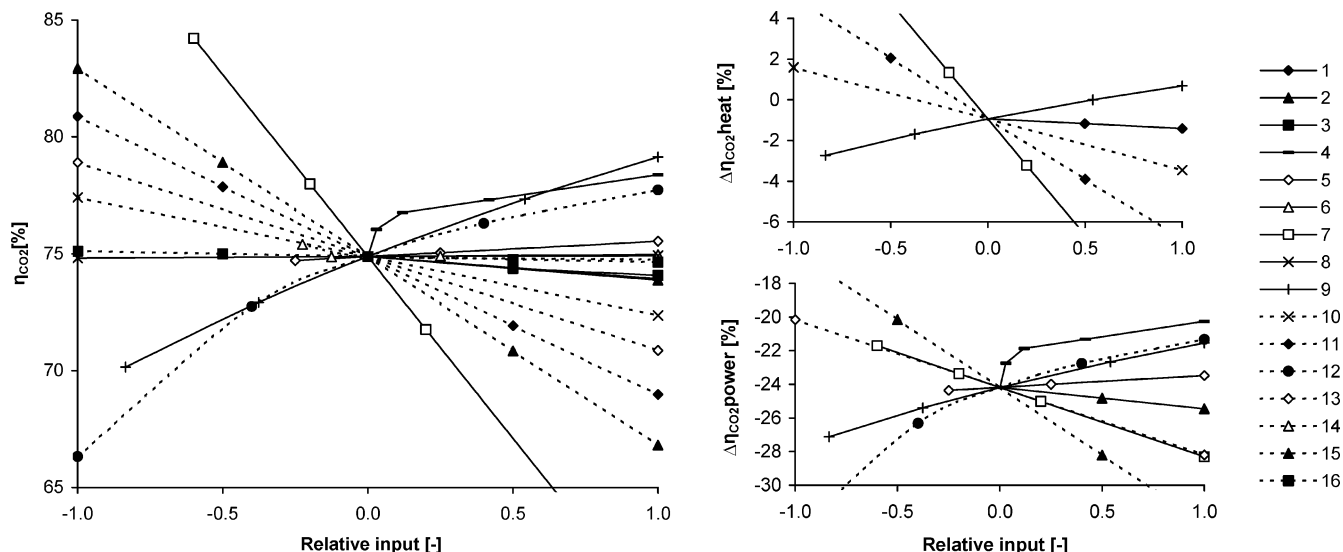
small. The overall heat balance of the process is slightly negative at these reactor conditions (see Section 3.3.4).

3.2. Steel Slag. Figure 4 shows the carbonation degree of steel slag in dependence of the reactor temperature, CO₂ pressure, and particle size on the basis of data presented earlier.⁷ In addition, the corresponding calculated CO₂ sequestration efficiencies are shown. The carbonation mechanisms of steel slag have been reported to be similar to those of wollastonite.⁴

Therefore, the influence of the three process variables on the carbonation degree and the CO₂ sequestration efficiency of both Ca-silicate feedstocks are generally similar. However, the differences in sequestration efficiency are smaller in the case of steel slag (Figures 3 and 4) as a result of the smaller differences in conversion due to its relatively rapid carbonation at mild process conditions.⁴ The limited set of data shown in Figure 4 suggests that, similarly to wollastonite, the energetically optimum reactor temperature is 200 °C. In addition, the optimum particle size also seems to be smaller than the minimum particle size of $<38 \mu\text{m}$ at which carbonation experiments were performed. However, the optimum CO₂ pressure seems to be lower than in the case of wollastonite, but this difference might be due to the lower temperature at which the measurements were performed (see also Figure 3).

The set of conversion data reported earlier for aqueous steel slag carbonation⁷ is too limited to determine a representative maximum CO₂ sequestration efficiency for this feedstock. In addition, the steel slag carbonation experiments were conducted at other sets of process conditions (particularly, reaction time and liquid-to-solid ratio) than the wollastonite carbonation experiments, which hinders the direct comparison of both feedstocks. An additional carbonation experiment with steel slag (batch S1) at the energetically optimum process conditions of wollastonite ($d < 38 \mu\text{m}$, $T = 200 \text{ }^\circ\text{C}$, $p_{\text{CO}_2} = 20 \text{ bar}$, $L/S = 5 \text{ kg/kg}$, $n = 500 \text{ rpm}$, and $t = 15 \text{ min}$) resulted in $\zeta_{\text{CaSiO}_3} = 67\%$ and $\eta_{\text{CO}_2} = 69\%$. The stream properties at these process conditions are shown in Figure 2, and the corresponding heat and power streams are shown in Table 4. At these process conditions, the energetic efficiency in the case of steel slag is significantly lower than that in the case of wollastonite. As Table 4 shows, this difference is particularly caused by a more negative overall reactor heat ($\Delta\eta_{\text{CO}_2} = -7$ vs -1% , for steel slag and wollastonite, respectively). Given that the conversions obtained for both feedstocks are similar, this effect is caused by the lower Ca content of the steel slag feedstock (i.e., 23 wt %⁷ vs 30 wt %⁴), which results in a larger amount of slurry that has to be heated to the reactor temperature (L/S ratio is kept constant).

It should be noted that the energetic efficiency of steel slag carbonation at the energetically optimum process conditions found for wollastonite (i.e., 69%) is not the maximum efficiency calculated for steel slag. The maximum efficiency at $<38 \mu\text{m}$ in Figure 4.I is 72% and that at 200 °C in Figure 4.II is even 73%. However, these values are based on carbonation degrees measured at a reaction time of 30 min instead of 15 min. A longer reaction time increases the conversion,⁷ while it has no direct effect on the energy consumption of the process, as taken into account in the current assessment. Therefore, a longer reaction time directly improves the energetic efficiency. The



#	Variable	Standard	Min	Max
1	Purge factor CO ₂ [-]	0 (0) ^a	0 (0)	1 (1)
2	Purge factor H ₂ O [-]	0 (0)	0 (0)	1 (1)
3	Temperature H ₂ O recycle [°C] ^b	40 (0)	40 (0)	80 (1) ^c
4	Pressure H ₂ O recycle [bar]	1 (0)	1 (0)	34.5 (1) ^d
5	Pressure drop reactor [bar]	1 (0)	0 (-0.25)	5 (1)
6	Excess gaseous CO ₂ supply reactor [%]	10 (0)	5 (-0.13)	50 (1)
7	L/S-ratio reactor feed [kg/kg] ^e	5 (0)	2 (-0.6)	10 (1)
8	Filter; solid content filter cake [kg/kg]	0.85 (0)	0.7 (-1)	1.0 (1)
9	Carbonation degree (ζ _{CaSiO₃}) [%]	69 (0)	60 (-0.83)	80 (1)
10	Heat of reaction (ΔH _r) [kJ/mol]	84 (0) ^f	64 (-1)	104 (1)
11	ΔT _{heat-exchanger} [°C]	20 (0) ^g	10 (-1)	30 (1)
12	Ore grade [%]	50 (0)	25 (-1)	75 (1)
13	Bond's working index [kWh/ton]	14 (0)	10 (-1)	18 (1)
14	Initial particle size feedstock [m]	0.1 (0)	0.01 (-0.2)	0.5 (1)
15	ε _{power} [kg/kWh] ^h	0.60 (0)	0.40 (-1)	0.80 (1)
16	ε _{heat} [kg/kWh]	0.20 (0)	0.15 (-1)	0.25 (1)

^a Numbers between brackets are the relative input values used for the graphs. ^b For these simulations, the ASPEN flowsheet was extended with a cooler, which cools the 'CO₂ REC 2' stream to 40 °C in order to avoid an increase of the gas volume that compressor 1 has to compress. ^c In principle, the maximum temperature of the H₂O recycle is T_{reactor}. However, this value could not be simulated because the process water is recycled at atmospheric pressure. ^d Maximum pressure = p_{reactor} - pressure drop over reactor. ^e In the sensitivity analysis the possible effect of the L/S-ratio on the conversion has been neglected. For wollastonite, a limited effect of the L/S-ratio was reported earlier.⁴ For steel slag, a reduction of the L/S-ratio seems to slightly increase the conversion measured at lab-scale.^{7,f} Heat of reaction as determined by ASPEN. ^g Temperature difference at the hot side of the heat exchanger. At the cold side of the heat exchanger the ΔT is slightly larger (e.g., 25 vs. 20 °C), since the reactor outlet slurry has a larger heat capacity than the reactor inlet slurry due to the presence of dissolved CO₂. ^h Representative values for a natural gas combined cycle and a powder coal power plant are 0.36 and 0.80 kg CO₂/kWh, respectively.¹⁷

Figure 5. Sensitivity analysis of CO₂ sequestration efficiency (η_{CO₂}) by wollastonite carbonation for the parameters shown in the table at energetically optimum reactor conditions (ζ_{CaSiO₃} = 69%, T = 200 °C, p_{CO₂} = 20 bar, d < 38 μm (batch W1)) and L/S = 5 kg/kg. In the graphs at the right, the energetic efficiency loss (Δη_{CO₂}) due to the heat and power consumption is shown for a selection of parameters.

optimum energetic efficiency of steel slag carbonation can only be determined on the basis of a more extensive set of carbonation experiments that fully takes into account the relatively rapid carbonation of this feedstock at mild process conditions.⁴

3.3. Sensitivity Analysis. Figure 5 shows the outcome of the sensitivity analysis on the CO₂ sequestration efficiency of wollastonite carbonation at energetically optimum reactor conditions. Most variables have a relatively small influence on the sequestration efficiency within the ranges studied (<1.5%). Eight variables have a relatively large influence on the energetic efficiency: the liquid-to-solid ratio, the specific CO₂ emission associated with power consumption, the temperature difference

at the hot side of the heat exchanger, the carbonation degree, the pressure of the water recycle, the Bond's working index, the ore grade, and the reaction heat assumed. Some of these factors will be discussed in more detail below.

3.3.1. Heat Exchanger Performance. The heat integration of the mineral carbonation process (particularly, the performance of the heat exchanger) has a large influence on the CO₂ sequestration efficiency, since the amount of heat both exchanged in the heat exchanger and cooled away in the cooler of the water recycle is large. At the energetically optimum reactor conditions and under the assumptions made, the heat generated by the carbonation reaction is smaller than the amount of heat required to heat up the reactants (Table 4). The energy

required to heat the reactor feed directly depends on the temperature difference assumed to be required for (cost-efficient) heat exchange between the reactor outlet and inlet slurries within the heat exchanger. For example, assuming a minimally feasible temperature difference in the heat exchanger of 10 °C, the CO₂ sequestration efficiency would increase to 81% and the process would generate a net surplus of reaction heat (253 kWh/(ton of CO₂ sequestered)) (for steel slag, 101 kWh/(ton of CO₂ sequestered) and $\eta_{\text{CO}_2} = 78\%$ at $\Delta T_{\text{heat-exchanger}} = 10$ °C). However, by reducing the driving force for heat exchange, the surface area required and, thereby, the investment costs of the heat exchanger would increase. Therefore, the optimum temperature difference can only be determined economically.

3.3.2. Liquid-to-Solid Ratio. A reduction of the *L/S* ratio leads to a substantial improvement of the heat balance of the process and, thus, the CO₂ sequestration efficiency (Figure 5 and Table 4). First, the energy required to pump and heat up the slurry is reduced. Second, less CO₂ has to be compressed by compressor 1 since less CO₂ dissolves into the slurry. Other possible energetic benefits, not taken into account in the present study, are a smaller reactor that has to be heated to the reactor temperature and the production of “less-diluted” heat by the exothermic carbonation reaction. Therefore, the aqueous mineral carbonation process should, in principle, be designed at the minimum feasible *L/S* ratio. However, if the *L/S* ratio becomes too low, pumping and stirring problems might arise because of an increased viscosity, which would result in a large decrease of the conversion.^{4,7} The minimum feasible *L/S* ratio depends on the final reactor and process design. The minimum *L/S* ratio that could be stirred adequately in the lab-scale autoclave reactor used for the carbonation experiments is 2 kg/kg.⁷ Reduction of the *L/S* ratio from 5 to 2 kg/kg (solids content of the reactor = 17 and 33 wt %, respectively) would increase the CO₂ sequestration efficiency by wollastonite carbonation to 84% (steel slag: $\eta_{\text{CO}_2} = 83\%$ at *L/S* = 2 kg/kg). Table 4 shows that, at *L/S* = 2 kg/kg, the process has a net surplus of reaction heat for both feedstocks. A dedicated industrial process might be operated at even lower *L/S* ratios down to 1 kg/kg, which may further improve the CO₂ sequestration efficiency of the process. Further experimental research in a continuous pilot-scale reactor is recommended to study the carbonation degree as a function of the *L/S* ratio and, thus, to determine the minimally feasible *L/S* ratio.

3.3.3. Water Recycle (Temperature and Pressure). The temperature of the water recycle has a remarkably small effect on the energetic efficiency of the process (Figure 5). The heat consumption of the heater is largely independent of the temperature of the water recycle because of the performance of the heat exchanger. However, it should be noted that, in the mineral carbonation process in Figure 2, the heat duty of the heat exchanger is very large (e.g., 3971 and 1690 kWh/(ton of CO₂ sequestered) at *L/S* = 5 and 2 kg/kg, respectively, for wollastonite). Thus, the investment costs for the heat exchanger may be substantial. Therefore, an increase of the water recycle temperature may be considered from an economic point of view.

In contrast to its temperature, the pressure of the water recycle does have a significant effect on the energetic sequestration efficiency. The water recycle is depressurized to 1 atm in order to enable filtration at atmospheric conditions and facilitate the addition of fresh feedstock to the slurry. By recycling the water at a higher pressure, less energy is required for pumping the slurry. In addition, less CO₂ in the CO₂ REC 2 stream has to be (re)compressed, since less CO₂ is released from the slurry upon depressurization. A relatively limited increase of the water

recycle pressure to 2 bar has the largest effect on the CO₂ sequestration efficiency without causing extra costs for high-pressure equipment.

3.3.4. Carbonation Reaction (Carbonation Degree and Reaction Heat). Obviously, the CO₂ sequestration efficiency depends strongly on the carbonation degree and, thereby, on the assumption that the conversion in the large-scale continuous reactor equals the conversion obtained in a lab-scale autoclave reactor (Section 2.3). At least two effects can be distinguished, which might cause a difference between these conversions.

First, the reactor type might affect the reaction rate because of physical effects (e.g., abrasion and mixing intensity). An increase of the carbonation degree of particularly coarse particles has been reported for Mg-silicates in a pilot-scale flow-loop reactor, compared to a laboratory autoclave reactor, probably because of intensified mixing and removal of the carbonation rate-limiting SiO₂-rim.⁵

Second, the carbonation degree might be influenced by the recycling of the process water. Preliminary experiments with regard to the effect of process water recycling on the carbonation of wollastonite and steel slag seem to suggest that the carbonation degree increases slightly because of process water recycling, possibly because of an increase of the ionic strength⁷ (Supporting Information). Given the major effect of the carbonation degree on the CO₂ sequestration efficiency, research on further enhancement of the carbonation process, while not decreasing the energetic efficiency, is warranted (see also Section 3.1).

In addition to the carbonation degree, the reaction heat assumed has a significant influence on the energetic efficiency (e.g., for steel slag, $\eta_{\text{CO}_2} = 66$ and 72% at $\Delta H_r = -64$ and -104 kJ/mol, respectively). Since both the composition and the occurring carbonation reactions have been simplified in the case of steel slag (see Section 2.1), further study to improve this input for the steel slag simulations, and thereby to increase the accuracy of the calculated CO₂ sequestration efficiencies, seems warranted. The carbonation of, for example, portlandite (Ca(OH)₂) ($\Delta H_r = -68$ kJ/mol⁹) present in fresh steel slag⁷ might cause the actual reaction heat to differ from the assumed one ($\Delta H_r = -84$ kJ/mol), which would then also change the energetic efficiency.

3.3.5. Grinding (Bond's Working Index and Ore Grade). Given the dominant effect of the energy consumption for grinding on the CO₂ sequestration efficiency (Table 4), the Bond's working index and ore grade are major influential parameters. Therefore, these parameters should be verified by measurements, to enable further improvement of the sequestration efficiency calculations.

3.4. Discussion. In the Supporting Information, a comparison of energetic efficiencies reported in this and other mineral carbonation studies is given. From the results of the other system study on aqueous mineral carbonation,⁵ a CO₂ sequestration efficiency for aqueous wollastonite carbonation of 82% can be deduced. It is difficult to directly compare the results of this study by the Albany Research Centre (ARC) with the present study because of the large number of different assumptions made in the assessment of the energetic efficiency.^{5,18} At a specific CO₂ emission of 0.85 (kg of CO₂)/kWh for a powder coal power plant and *L/S* = 2.33 kg/kg as used in the ARC study,⁵ our model resulted in a slightly lower CO₂ sequestration efficiency of 75%. This difference is particularly caused by the recycling of nonconverted solid feedstock as applied in the ARC study.^{5,18} The possible separation and recycling of nonconverted feedstock present in the reactor outlet might cause a substantial increase

of the CO₂ sequestration efficiency. However, the feasibility of continuous large-scale separation of noncarbonated and carbonated Ca-silicate particles is presently unclear (see discussions in earlier work^{2,4}). Further research on this subject is warranted.

In determining the CO₂ sequestration efficiency of the entire sequestration process (Figure 1), it should be kept in mind that, in system studies on CO₂ capture technologies, compression is typically (already) included, since CO₂ has to be compressed for transportation (typically, $p > 80$ bar).³ The maximum CO₂ sequestration efficiency of the aqueous wollastonite carbonation process, without the energy consumption due to compression of the CO₂ feed, is 82 and 90% at $L/S = 5$ and 2 kg/kg, respectively (steel slag: $\eta_{\text{CO}_2} = 73$ and 87%, respectively). In addition, the lower CO₂ pressure required for the aqueous carbonation of Ca-silicates, compared to other CO₂ storage options, such as storage in depleted gas fields, as well as Mg-silicate carbonation processes (both, typically, $p > 100$ bar^{3,5}), may give an energetic benefit that should be taken into account when comparing different CO₂ storage technologies.

Overall, application of the process conditions used for lab-scale carbonation experiments would lead to a mineral carbonation process that would consume a substantial amount of extra energy ($\Delta\eta_{\text{CO}_2} \approx 25\text{--}30\%$). However, the CO₂ sequestration efficiency of aqueous Ca-silicate carbonation might substantially improve if the options that are identified in this study could be implemented. Therefore, pilot-scale research on mineral carbonation is recommended to determine the feasibility of the suggested reduction of the L/S ratio, and to verify the energetic efficiency calculations with respect to the carbonation degree. In addition, a cost evaluation study on CO₂ sequestration by aqueous mineral carbonation is required for final optimization of the process conditions (including reaction time) and the heat integration of the process. Final assessments of the energetic feasibility of CO₂ sequestration by mineral carbonation should be made for specific locations (particularly, with respect to ϵ_{power}) and should include the energy consumption of (possible) CO₂ capture, mining, and transportation.

4. Conclusions

Increasing the carbonation rate of wollastonite or steel slag by either grinding the feedstock, elevating the reaction temperature, or increasing the CO₂ partial pressure was shown to also improve the energetic CO₂ sequestration efficiency. Within the ranges of process conditions studied, energetic optima were found between the carbonation degree and the associated extra energy consumption, for both the temperature and the CO₂ pressure. The maximum CO₂ sequestration efficiency for wollastonite at a liquid-to-solid ratio of 5 kg/kg and a reaction time of 15 min was 75% at 200 °C, 20 bar CO₂, and a particle size of $< 38 \mu\text{m}$. The grinding of the feedstock ($\Delta\eta_{\text{CO}_2} = -15\%$) and the compression of the carbon dioxide (-7%) were identified as the main energy-consuming process steps. At these process conditions, a significantly lower CO₂ sequestration efficiency was found for steel slag, 69%, mainly due to the lower Ca content of the feedstock. Further grinding (particularly, wollastonite) or reducing the CO₂ partial pressure (steel slag) can potentially improve the CO₂ sequestration efficiency. In addition, a sensitivity analysis has shown that the CO₂ sequestration efficiency may be increased substantially by, e.g., improving the heat integration of the process and reducing the amount of process water applied. The options that have been identified to improve the energetic efficiency warrant a further

assessment of the (energetic) feasibility of CO₂ sequestration by aqueous mineral carbonation on the basis of a pilot-scale process.

Acknowledgment

The authors thank Robin Hink for laying down a basis for the process studies presented. Jan-Wilco Dijkstra is acknowledged for his help with the ASPEN simulations. This research was funded by the Dutch Ministry of Economic Affairs as part of the energy research program of ECN.

Supporting Information Available: The Supporting Information contains additional details on process water recycling, CO₂ loss, and comparison of energetic efficiencies reported for mineral carbonation processes. This material is available free of charge via the Internet at <http://pubs.acs.org>.

Notation

Symbols

CO_{2,avoided} = net amount of CO₂ avoided, ton/h
 CO_{2,sequestered} = amount of CO₂ sequestered in reactor, ton/h
 d = particle size, m
 $D[4,3]$ = volume-based mean particle size, m
 d_0 = initial particle size, m
 d_1 = final particle size, m
 E = energy consumption, kWh
 E_{heat} = heat consumption, kWh
 E_{power} = power consumption, kWh
 L/S = liquid-to-solid ratio, kg/kg
 n = stirring rate, rpm
 p = total reactor pressure, bar
 p_{CO_2} = CO₂ partial pressure, bar
 $p_{\text{H}_2\text{O}}$ = H₂O partial pressure, bar
 T = (reactor) temperature, °C
 t = reaction time, min
 TIC_0 = total inorganic carbon content in fresh feedstock, wt %
 W = energy consumption by grinding, kWh/ton feedstock
 W_i = Bond's work index, kWh/ton feedstock
 ΔG_r = Gibbs energy of reaction, kJ/mol
 ΔH_r = reaction enthalpy, kJ/mol
 Δp = pressure drop, bar
 ΔT = temperature difference hot-side heat exchanger, °C
 $\Delta\eta_{\text{CO}_2}$ = CO₂ sequestration efficiency loss, %
 ϵ_{heat} = specific CO₂ emission heat, kg/kWh
 ϵ_{power} = specific CO₂ emission power, kg/kWh
 ζ = conversion/carbonation degree, %
 ζ_{Ca} = conversion based on calcium content in feedstock, %
 ζ_{CaSiO_3} = conversion based on CaSiO₃ in reactor inlet, %
 η_{CO_2} = energetic CO₂ sequestration efficiency, %

Literature Cited

- Wu, J. C. S.; Sheen, J.-D.; Chen, S.-Y.; Fan, Y.-C. Feasibility of CO₂ fixation via artificial rock weathering. *Ind. Eng. Chem. Res.* **2001**, *40*, 3902–3905.
- Huijgen, W. J. J.; Comans, R. N. J. (Energy Research Centre of The Netherlands). *Carbon dioxide storage by mineral carbonation*; Report 2005/11; International Energy Agency—Greenhouse Gas R&D Programme (IEA GHG): Cheltenham, U.K., 2005.
- IPCC. *IPCC special report on carbon capture and storage*; Metz, B., Davidson, O., Coninck de, H. C., Loos, M., Meyer, L. A., Eds.; Cambridge University Press: Cambridge, U.K., and New York, U.S.A., 2005.

- (4) Huijgen, W. J. J.; Witkamp, G. J.; Comans, R. N. J. Mechanisms of aqueous wollastonite carbonation as a possible CO₂ sequestration process. *Chem. Eng. Sci.* **2006**, *61*, 4242–4251.
- (5) O'Connor, W. K.; Dahlin, D. C.; Rush, G. E.; Gerdemann, S. J.; Penner, L. R.; Nilsen, D. N. *Aqueous mineral carbonation: Mineral availability, pretreatment, reaction parameters and process studies*; DOE/ARC-TR-04-002; Albany Research Center: Albany, OR, 2005.
- (6) O'Connor, W. K.; Dahlin, D. C.; Rush, G. E.; Dahlin, C. L.; Collins, W. K. Carbon dioxide sequestration by direct mineral carbonation: process mineralogy of feed and products. *Miner. Metall. Process.* **2002**, *19*, 95–101.
- (7) Huijgen, W. J. J.; Witkamp, G. J.; Comans, R. N. J. Mineral CO₂ sequestration by steel slag carbonation. *Envi. Sci. Technol.* **2005**, *39*, 9676–9682.
- (8) Iizuka, A.; Fujii, M.; Yamasaki, A.; Yanagisawa, Y. Development of a new CO₂ sequestration process utilizing the carbonation of waste cement. *Ind. Eng. Chem. Res.* **2004**, *43*, 7880–7887.
- (9) Lackner, K. S.; Wendt, C. H.; Butt, D. P.; Joyce, E. L.; Sharp, D. H. Carbon dioxide disposal in carbonate minerals. *Energy* **1995**, *20*, 1153–1170.
- (10) Huijgen, W. J. J.; Comans, R. N. J. Carbonation of steel slag for CO₂ sequestration: Leaching of products and reaction mechanisms. *Envi. Sci. Technol.* **2006**, *40*, 2790–2796.
- (11) Teir, S.; Eloneva, S.; Zevenhoven, R. Production of precipitated calcium carbonate from calcium silicates and carbon dioxide. *Energy Convers. Manage.* **2005**, *46*, 2954–2979.
- (12) Kakizawa, M.; Yamasaki, A.; Yanagisawa, Y. A new CO₂ disposal process using artificial rock weathering of calcium silicate accelerated by acetic acid. *Energy* **2001**, *26*, 341–354.
- (13) *Aspen Plus 2004.1*; Aspen Technology Inc.: Cambridge, MA, 2005.
- (14) Carlson, E. C. Don't gamble with physical properties for simulations. *Chem. Eng. Prog.* **1996**, *92*, 35–46.
- (15) Bond, F. C. Crushing and grinding calculations. Part I. *Br. Chem. Eng.* **1961**, *6*, 378–385.
- (16) Perry, R. H.; Green, D. W. *Perry's Chemical Engineers' Handbook*; McGraw-Hill: New York, 1998.
- (17) Rubin, E. S.; Rao, A. B.; Chen, C. Comparative assessments of fossil fuel power plants with CO₂ capture and storage. In *Proceedings of the 7th International Greenhouse Gas Technology Conference*, Vancouver, BC, Canada, 2004; Rubin, E. S., Keith, D. W., Gilboy, C. F.; Elsevier: New York, 2005; Vol. I, pp 285–293.
- (18) Nilsen, D. N.; Penner, L. R. *Reducing greenhouse gas emissions: engineering and cost assessment of direct mineral carbonation technology (process development information for the olivine process)*; DOE/ARC-TR-01-015; Albany Research Center: Albany, OR, 2001.

Received for review May 22, 2006

Revised manuscript received September 13, 2006

Accepted September 20, 2006

IE060636K